

THE EVOLUTION OF THE MASS-METALLICITY RELATION UP TO $Z \approx 0.9$ FROM THE VIMOS/VLT DEEP SURVEY

F. Lamareille^{1,2}, T. Contini¹, S. Charlot^{2,3}, J. Brinchmann^{2,4} and the VVDS team

Abstract. We present the first results derived from the spectrophotometric properties of the VIMOS VLT Deep Survey (VVDS) first epoch data. We have measured the spectral features (emission/absorption lines, 4000Å break) of a sample of ≈ 8000 galaxies taken from the VVDS deep 02h and CDFS fields using the platefit_VVDS pipeline. After selecting a sub-sample of star-forming galaxies based on emission-line ratios, the gas-phase oxygen abundances have been derived by fitting all available emission lines with photo-ionization models. Finally the masses have been derived by fitting all photometric points together with significant spectral features to a library of stellar population models with complex star formation histories. The mass-metallicity relation that we find at low redshift is in good agreement with previous studies performed in the local Universe. Moreover we find a significant evolution of the mass-metallicity relation with the redshift, the galaxies having on average less metals at a given mass when the redshift increases. We also find a flattening of the mass-metallicity relation up to $z \sim 1$.

1 Introduction

The stellar mass and the gas-phase metallicity of a galaxy are two of the main parameters involved in the study of galaxy formation and evolution. They indeed serve as cosmological clocks for the two main processes which drive the evolution of a galaxy: respectively the star formation history and the metal enrichment. These two processes are linked together in the simple close-box model by the physics of stars and interstellar clouds. This link is characterized by the yield y , which is a physical constant, as shown in the following equation where Z is the metallicity, M_\star the stellar mass, and M_g the gas mass:

$$Z = y \times \ln \left(1 + \frac{M_\star}{M_g} \right) \quad (1.1)$$

Thus, still in the close-box model for which the total mass of the galaxy remains constant, the stellar-mass-metallicity (hereafter mass-metallicity) relation is simply driven by the progressive enrichment of the interstellar medium as long as new generations of stars are formed: the massive short-lived stars produce the metals and the dwarf long-lived stars contribute to the increase of the stellar mass.

However, many studies have now shown that the close-box model is much too simple to reproduce galaxy evolution. We know indeed that the merging of galaxies is playing a major role in the increase of the stellar mass, so that the total mass of a galaxy does not stay constant. Moreover, the stellar winds, supernovae and AGN feedbacks are responsible of metal loss into the intergalactic medium. We also know that accretion of gas is playing a major role in evolution of galaxies. These effects prevent the metallicity to increase as described in equation 1.1. We need instead to define an effective yield y_{eff} . The effective yield is an indicator of both metal loss and dry accretion of primordial gas. The smaller is the effective yield, the flatter is the mass-metallicity relation.

¹ Laboratoire d'Astrophysique de Toulouse/Tarbes (UMR5572), CNRS, Université Paul Sabatier - Toulouse III, Observatoire Midi-Pyrénées, 14 av. E. Belin, 31400 Toulouse, France

² Max-Planck Institut für Astrophysik, 85741 Garching, Germany

³ Institut d'Astrophysique de Paris (UMR7095), CNRS, 98bis Bd. Arago, 75014 Paris, France

⁴ CAUP, Rua das Estrelas S/N, 4150-752 Porto, Portugal

First discovered with irregular galaxies, the mass-metallicity relation has been extensively studied so far and is now well established in the local universe by the works of Tremonti et al. (2004) with SDSS data and Lamareille et al. (2004) with 2dFGRS data, the later done on the luminosity-metallicity relation which is easier to derive when small number of photometric bands are available. These two studies have shown in two different ways that the mass-metallicity is mainly driven by the decrease of metal loss when stellar mass increases: first by the increase of the effective yield, or by the increase of the slope of the mass-metallicity relation. The later effect has also been confirmed recently by Lee et al. (2006) on SDSS data.

At least two processes are able to explain the decrease of metal loss when stellar mass increases. The first is the joint increase of the total mass of the galaxies together with their stellar mass, as predicted by the hierarchical model. This process ends up to galaxies with a small stellar mass having also a small gravitational potential and not being able to retain their metals. The second process is the downsizing effect: massive galaxies have less star-forming activity, and thus eject less metals in the intergalactic medium.

The evolution of the mass-metallicity - or luminosity-metallicity - relation up to $z \sim 1$ has been already intensively studied but on small samples (Hammer et al. 2005; Kobulnicky et al. 2003 among others). Recent studies have been performed on larger samples (> 100 galaxies) but with contradictory results. Savaglio et al. (2005) found a steeper slope in the distant universe and interpreted these results in the framework of the close-box model. On the contrary, Lamareille et al. (2006b) have not found any significant evolution of the slope of the luminosity-metallicity relation, while the average metallicity at $z \approx 0.9$ is lowered by 0.55 dex at a given luminosity, and by 0.28 dex after correction for luminosity evolution. At higher redshifts ($z \sim 2.0$), Erb et al. (2006) have found a flatter mass-metallicity relation which is also lowered in metallicity by 0.56 dex compared to the local estimate.

2 Description of the sample

The VIMOS/VLT Deep Survey (VVDS; Le Fèvre et al. 2005) is one of the widest and deepest spectrophotometric surveys of distant galaxies with a mean redshift of $z \approx 0.7$. The optical spectroscopic data obtained on VIMOS at ESO/VLT offer a great opportunity to study the evolution of the mass-metallicity relation on a statistically significant sample up to $z \approx 0.9$. This upper limit in redshift is imposed by the emission lines needed to compute a metallicity being redshifted out of the wavelength range of the survey.

For this analysis, we used the first epoch data of the two VVDS deep fields (VVDS-02h and CDFS). The deep selection function of the VVDS is very simple: $I_{AB} < 24$. Nevertheless, we had to add some other selection criteria in order to calculate the stellar mass and the metallicity accurately. We kept only objects with a redshift known at more than 75% confidence level (i.e. VVDS redshift flags 2, 3 and 4), and we removed all stars and broad-line AGNs. The emission lines have been measured with the platefit_VVDS pipeline, which accurately fits all emission lines after removing the stellar continuum and absorption lines (see Lamareille et al. 2006a, for a description of the quality tests). Note that because of the limited wavelength coverage of the spectra, we do not observe all classical optical lines at all redshifts.

The narrow-line AGNs are removed using standard emission-line diagnostics, i.e. Kewley et al. (2001) in the interval $0.2 < z < 0.4$ with $H\alpha$, $H\beta$, [OIII]5007, [NII]6584 and [SII]6717,6731 observed; and Lamareille et al. (2004) in the interval $0.5 < z < 0.9$ with $H\beta$, [OIII]5007 and [OII]3727 observed. For the other redshift ranges, we use a minimum classification based on $H\alpha$, [NII]6584 and [SII]6717,6731 at $0.0 < z < 0.2$ and on $H\beta$ and [OIII]5007 at $0.4 < z < 0.5$.

2.1 Estimation of the stellar masses

The stellar masses are estimated by comparing the observed SED, and two significant spectral features ($H\delta$ absorption line and D4000 break), to a library of stellar population models. The models are based on Bruzual & Charlot (2003) models with some improvements, such as secondary bursts added to the standard declining exponential SFH. The main result of the inclusion of secondary bursts, compared to previous methods which adopted a smooth SFH is to get somewhat higher masses as we are now able to better reproduce the colors of galaxies with both old and recent stellar populations (see Pozzetti et al. in prep. for a discussion on the different methods). In this study we use the standard Λ CDM cosmology, i.e. $h = 0.7$, $\Omega_m = 0.3$ and $\Omega_\Lambda = 0.7$.

The SED of the models are compared to all photometry available, i.e. mainly CFH12k *BVRI* and CFHTLS *ugriz* bands, and *JK* photometry available for some objects. The χ^2 of each model are summarized in a PDF

(Probability Distribution Function) of the stellar mass, given the library of models, which is described for each mass bin by the sum $\sum \exp(-\chi^2(M_\star)/2)$. Our stellar mass estimate is given by the median of the PDF. This method allows us to get a reliable estimate which takes all possible solutions into account and not only the best-fit. It also allows us to get an error estimate from the width of the PDF (see Brinchmann et al. 2004, for a discussion on the bayesian approach).

In order to study the evolution of the mass-metallicity relation, we define three volume-limited samples at different redshift ranges: $0.0 < z < 0.5$, $0.5 < z < 0.7$ and $0.7 < z < 0.9$. We avoid volume corrections by defining three limiting masses, as the minimum stellar mass for which a galaxy remains visible in the whole redshift range, given the selection function. The mass limits are respectively 8.45, 8.81 and 9.08 in logarithm of solar masses.

2.2 Estimation of the metallicities

We estimate the metallicities, as the gas-phase oxygen abundance $12 + \log(\text{O}/\text{H})$, using again a bayesian approach. The fluxes of all measured emission lines are compared to a set of photoionization models, which predict the theoretical flux ratios given four parameters: the gas-phase metallicity, the ionization level, the dust-to-metal ratio and the reddening (Charlot & Longhetti, 2001).

In many cases, especially at high redshifts where nitrogen and sulfur lines are not observed, the metallicity is degenerate because of radiative cooling at high metallicities which lowers the intensity of oxygen lines. We solve the degeneracy by keeping in the PDF the one of the two peaks with the highest probability. For the following analysis, we keep only the objects for which the metallicity is estimated with an uncertainty lower than 0.25 dex.

3 Discussion

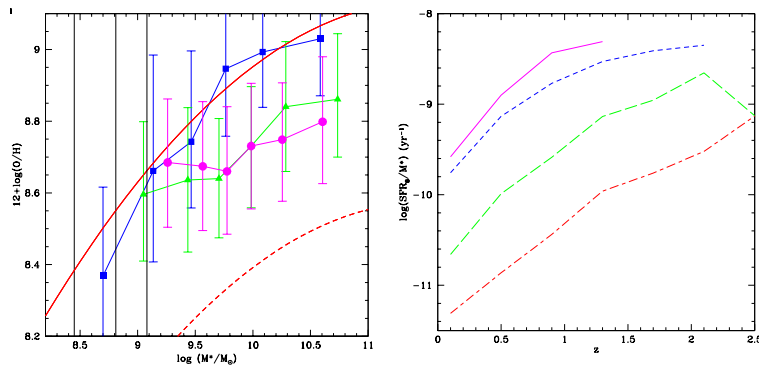


Fig. 1. *Left:* Evolution of the mass-metallicity relation. This diagram presents the relation between gas-phase metallicity and stellar mass for VVDS galaxies as a function of redshift. Each point is calculated as the running median of the metallicity of the galaxies in the sample along the stellar mass axis. The squares, the triangles and the circles stand respectively for the $0.0 < z < 0.5$, $0.5 < z < 0.7$ and $0.7 < z < 0.9$ redshift ranges. The curves show the Tremonti et al. (2004) and Erb et al. (2006) results as solid and dashed lines respectively. The vertical lines show the three mass limits of the subsamples. *Right:* This diagram shows the mean specific star formation rates of VVDS galaxies as a function of redshift in four stellar mass ranges: $8 < \log(M_\star) < 9$ (solid line), $9 < \log(M_\star) < 10$ (short-dashed line), $10 < \log(M_\star) < 11$ (long-dashed line) and $11 < \log(M_\star) < 12$ (short-dashed long-dashed line). The specific star formation rates have been derived from SED fitting with the same method as for stellar masses described in text.

We evaluate the shape of the mass-metallicity relation in each redshift range by calculating a running median of the metallicity along the stellar mass axis. This approach is justified by the low uncertainties of the stellar masses (~ 0.1 dex) compared to the metallicities (~ 0.2 dex). Moreover, it allows a direct comparison with previous studies (Tremonti et al. 2004; Erb et al. 2006) which use the same method.

Figure 1 (left) shows the results for each subsample defined above. We see that our nearest to local estimate (redshift range $0.0 < z < 0.5$) is in good agreement with SDSS data. In the $0.5 < z < 0.7$ redshift range, we see

a clear flattening of the mass-metallicity relation, mainly driven by a stronger evolution of its high-mass end. The $0.7 < z < 0.9$ redshift range shows a similar trend.

The flattening of the mass-metallicity relation can be understood in a simple open-to-close box model: low stellar mass galaxies would evolve more like an open-box model with a very low effective yield, while massive galaxies would evolve more like a close-box model with an effective yield close to the true yield value. In the open-to-close box model, the higher is the stellar mass the stronger is the evolution of the metallicity each time the galaxy is forming stars (i.e. each time its stellar mass increases).

The open-to-close box model assumes an increase of the effective yield with stellar mass. The flattening of the mass-metallicity relation is thus an evidence of the hierarchical mass assembly as the gravitational potential of the galaxies does not remain constant during the star formation process.

We calculate that galaxies at $\log(M_\star) \sim 10.5$ show a decrease of 0.26 dex in metallicity up to $z \approx 0.8$. We thus find that the metallicity doubles in 8.54 Gyr, in very good agreement with both Lamareille et al. (2006b) and Erb et al. (2006) who found that the metallicity doubles in 8.87 Gyr and 8.95 Gyr respectively. For galaxies at $\log(M_\star) \sim 9.5$, the decrease is only of 0.15 dex, The metallicity of these galaxies doubles in 10.15 Gyr, whereas lower mass galaxies show higher specific star formation rates.

It is interesting to note that the flattening effect we have found around $z \sim 1$ is stronger than the one noticed by Erb et al. (2006) at $z \sim 2$, who found a similar slope as in the local universe. What process could explain a re-steepening of the mass-metallicity relation in the $1 < z < 2$ redshift range? The downsizing effect may be an answer. Indeed, we know that the more massive are the galaxies, the quicker their star formation activity rises to a maximum at higher redshifts. As shown in Fig. 1 (right), galaxies at $\log(M_\star) \sim 9.5$ reach a maximum around $z \sim 1.5$, the ones at $\log(M_\star) \sim 10.5$ around $z \sim 2$. This effect can explain why the firsts would have produced more metals from $z = 2$ to $z = 1$ than from $z = 1$ to $z = 0$, while the seconds stay at a constant rate.

4 Conclusion

We have derived stellar masses and metallicities of VVDS galaxies up to $z = 0.9$ and studied the evolution of the median mass-metallicity relation in three redshift bins. We have found a flattening of the mass-metallicity relation at $z \sim 1$ which is explained in the open-to-close box model. Our results for the high-mass end of the mass-metallicity relation are in very good agreement with previous studies either at $z \sim 1$ or at $z \sim 2$, showing that the metallicity of these galaxies would double in ≈ 8.6 Gyr. For intermediate-mass galaxies, we have found a smaller evolution from $z = 1$ to $z = 0$ than from $z = 2$ to $z = 1$, comparing our results both to local and high redshifts studies. This can be explained by the downsizing effect which tells us that these galaxies reached a maximum in their star formation activity between $z = 1$ and $z = 2$.

The study of the evolution of the mass-metallicity relation can be improved in two ways: first by including galaxies with lower stellar mass at intermediate redshifts ($z < 1$), second by observing in their near-infrared galaxies at higher redshifts ($z > 1$) in order to estimate their metallicities (on-going program using SINFONI at VLT).

References

- J. Brinchmann, S. Charlot, S. White, et. al., 2004, MNRAS, 351, 1151
 Bruzual G., Charlot S., 2003, MNRAS, 344, 1000
 Charlot S., Longhetti M., 2001, MNRAS, 323, 887
 Erb D., Shapley A., Pettini M., et al., 2006, ApJ, 644, 813
 Hammer F., Flores H., Elbaz D., et al., 2005, A&A, 430, 115
 Kewley L., Heisler C., Dopita M., Lumsden S., 2001, ApJS, 132, 37
 Kobulnicky H., Willmer C., Phillips A., et al., 2003, ApJ, 599, 1006
 Lamareille F., Mouhcine M., Contini T., Lewis I., Maddox S., 2004, MNRAS, 350, 396
 Lamareille F., Contini T., Le Borgne J.-F., et al., 2006a, A&A, 448, 893
 Lamareille F., Contini T., Brinchmann J., et al., 2006b, A&A, 448, 907
 Lee H., Skillman E., Cannon J., et al., 2006, ApJ, 647, 970
 Le Fèvre O., Vettolani G., Garilli B., et al., 2005, A&A, 439, 845
 Savaglio S., Glazebrook K., Le Borgne D., et al., 2005, ApJ, 635, 260
 Tremonti C., Heckman T., Kauffmann G., et al., 2004, ApJ, 613, 898